

Meeting of the plasma physics division of the
american physical society
Boston, MA (USA)
CEA-CONF--7709

29 Oct - 2 Nov 1984

SOFT X-RAY IMAGING WITH AXISYMMETRIC MICROSCOPE AND ELECTRONIC READOUT

A. Sauneuf, C. Cavaller, Ph. Henry, J. Launspach,
J. de Mascureau, M. Rostaing

Commissariat à l'Energie Atomique, Centre d'Etudes de Limeil-Valenton
B.P. n° 27, 94190 Villeneuve-Saint-Georges, France

Abstract

An axisymmetric microscope with 10 X magnification has been constructed ; its resolution has been measured using several grids, backlighted by an X-ray source and found to be near 25 μm . So it could be used to make images of laser driven plasmas in the soft X-ray region. In order to see rapidly those images we have associated it with a new detector. It is a small image converter tube with a soft X-ray photocathode and a P20 phosphor deposited on an optic fiber plate. The electronic image appearing on the screen is read by a CCD working in the spectral range. An electronic image readout chain, which is identical to those we use with streak cameras, then processes automatically and immediately the images given by the microscope.

Introduction

Investigating the laser-driven plasmas requires the formation and detection of images in the soft X-ray region (from about 100 eV to some keV). We have worked into image formation by grazing specular reflection and taken up the construction and use of an axisymmetric microscope (Wolter microscope)¹⁻². Furthermore we have looked for replacing the film, rather uneasy to handle, by a detector made of an image converter tube (ICT) and an electronic readout using a charge coupled device (CCD). Figure 1 shows the schematic representation of the apparatus made of all these devices and its use on an laser-matter interaction chamber.

Axisymmetric microscope

Principle and characteristics

This optics consists of hyperboloid and ellipsoid mirrors that are coaxial and confocal surfaces of revolution. Owing to the well-known properties of conics, the system is stigmatic for the other two foci F_H (object-point) and F_E (image point). It is also nearly aplanetic near these points since ABBE's relation, $\sin \phi_H / \sin \phi_E = \text{constant}$, is almost achieved if ϕ_H variation is small. Then the theoretical resolution can be better than $2 \mu\text{m}$ within an object field of $300 \mu\text{m}$ radius, which is good enough for the plasmas we are studying³⁻⁴. Moreover the diffraction does not limit this resolution even for soft X-rays (energy $> 100 \text{ eV}$).

The shape and the dimensions of both mirrors are calculated from the input parameters : the magnification, the object-microscope distance, the collecting angle, and the average grazing angle on each surface. This last parameter takes into account the surface material and the X-ray cut-off energy.

The characteristics of our microscope are as follows :

Object-microscope distance : $P = 50 \text{ mm}$

Magnification : $G = 10$

Object-image distance : $D = 746 \text{ mm}$

Total length : 35 mm

Diameters : • front section (H) : 11.5 mm

• intersection : 14.3 mm

• rear section (E) : 15 mm

Mean grazing angles (the object is supposed to be the point F_H)

• at the borders : 1.8 degree

• at the intersection : $1.44 \text{ degree (on H)}$

$1.89 \text{ degree (on E)}$.

Incident beam :

- within two cones of half-angle ϕ_H : 6.06 and 6.55 degree
- collecting solid angle : 6×10^{-3} steradian

Band pass : 0 - 1.7 keV (nickel cut-off energy is 1.7 keV).

A metallic circular disk placed in front of the microscope prevents direct rays from reaching the image zone.

Dimensional measurements

That microscope has been made by SAGEM* with the following steps :

- diamond turning of an aluminum alloy mandrel on a high stability lathe ;
- electroplating of a thick nickel layer (about .8 mm) on that mandrel ;
- chemical dissolution of the mandrel ;
- assembling the nickel part on a stand which allows us to fix the obscuration cap.

The shape and roughness of the surfaces were measured with an electronic analyser accurate to 200 Å. On azimuthal contours, the deviation from roundness remains inferior to .3 μm . On saggital contours, we notice undulations ; their wavelengths lay within 20 to 500 μm and their amplitude remains inferior to .2 μm . Nevertheless local slope variations may reach 10^{-3} radian and lower the resolution.

* SAGEM, 6 avenue d'Iena, 75783 PARIS Cedex 16, FRANCE.

Spatial resolution

It was evaluated by recording on an X-ray film the image of metallic grids backlighted by visible light or by X-rays. These grids have a periodicity of 86 - 60 - 40 - 25 - 12.7 μm and are made of gold or silver thick enough ($\approx 5 \mu\text{m}$) so that the absorption of the concerned X-rays is very high (spectral band width : 1 to 1.7 keV).

Figure 3 shows that visible light resolution is about 10 μm whereas X-ray resolution is limited to 25 μm . The difference may be due to the surface unmodulations, the dimensions of which are small compared to the visible light wavelength and very large in the X-ray field.

Pulsed X-ray tests

This microscope may be used to study some laser-driven plasmas. It takes place in the same mechanical device as those of pinhole cameras which allows the microscope axis to be into straight line with the plasma center by means of adjusting knobs and use of visible light.

For these tests we used an X-ray film (Kodirex or DF5) protected from visible lights by an aluminum sheet which also acted as an X-ray attenuator.

In order to compare its performances to those of a pinhole camera having the same magnification, the microscope and the pinhole camera were placed as shown in figure 4. The target was a copper wire (diameter 250 μm) irradiated by two laser beams delivering an average energy of 5 J in a 50 ps pulse FWHM. Such a configuration gives two plasmas then two separate X-ray sources.

A streak camera (TSN 506 X) recorded at the same time the X-ray pulse duration.

The microscope reflecting surfaces were protected by a 1.5 μm mylar sheet from the target debris and the 15 μm diameter pinhole was screened by a 25 μm Be sheet.

Figure 5 shows the images of the two X-ray sources given by both devices and a typical streak camera record.

As it takes quite a long time to process X-ray film and make measurements on it, we tried to replace it by a CCD camera. First we successfully put a CCD in a pinhole camera⁵ but CCD are not sensitive to X-rays lower than 1 keV and, in the soft X-ray region, pinhole cameras are diffraction limited. So we thought of using an image converter tube to transform the images given by the Wolter microscope.

Image converter tube

Principle and experimental set-up

It is derived from an electrostatically focused diode-inverter tube which is made by RTC^{*} and works in visible light. For our needs, such a tube has been modified as follows (figure 1) :

- in order to collect more light, the output glass window is replaced by an optic fiber plate on which is deposited the P10 phosphor screen ;
- the input glass window is replaced, by a mechanical device which holds a soft X-ray photocathode (a very thin Au or CsI layer on a plastic foil as transparent as possible) ; that photocathode is entirely under vacuum ;
- a vacuum flange with an elastomer O-ring is added to the front part to allows pumping of the tube and good X-ray transmission.

An insulating adaptor connects the tube to the microscope so that the photocathode is in the image plane. The tube axis makes a slight angle with the microscope axis to prevent unabsorbed X-rays from illuminating the electronic image zone on the screen.

* RTC, 130 avenue Ledru-Rollin, 75540 Paris Cedex 11, France.

The photocathode is grounded and a voltage of +10 kV is put on the screen. The external face of the optic fiber plate is metallized and grounded in order to protect detectors using CCD.

Tests with a continuous X-ray source

First, the ICT and its adaptor were mounted on a test chamber coupled with a classical X-ray tube having a Cr anode and a 800 μm Be window. The X-ray spectrum is comprised between 2.5 keV and U keV (U is the voltage applied to the tube and may be adjusted from 10 to 17 kV). As the ICT was sensible to that light, we put a 75 μm grid in front of and against the photocathode. The visible light image was then recorded on a 55 PN Polaroid film (figure 6).

We can see two parts on that image. The very luminous small diameter spot corresponds to the direct X-rays which are not absorbed by the photocathode. The other spot is the electronic image of the grid and we can notice the absence of distorsion though the photocathode is plane instead of being spherical. But the small difference of shape may explain the defocusing of the image center. So we have to find a better position of the photocathode to achieve a good resolution over the whole field and we expect a 8 to 10 $\mu\text{p/mm}$ resolution.

Tests on an interaction chamber

As the resolution is far better than that of the axisymmetric microscope (4 $\mu\text{p/mm}$ on the image) we have put the ICT on the microscope holding device. Still with Polaroid film we have recorded images similar to those first obtained on X-ray film. Figure 7 shows such a record on which the direct X-rays level seems very low so the apparatus could be made more simple.

In comparison with X-ray film, the sensitivity has been increased but film is not a linear detector. So we have replaced it by a CCD camera coupled to an analog-digital converter. That camera uses a THOMSON-CSF TH31113 CCD and its input optic fiber plate is applied on the ICT output⁶. The signal is then send to the Pericolor 1000 system which allows image processing and storage on disquettes as well as immediate viewing.

Figure 8 shows the whole apparatus mounted on the interaction chamber ASTARTE. Figures 9a and 9b shows the same image of a double plasma with two different processes.

Conclusion

In the soft X-ray region, we can see the interest of associating an ICT and a CCD camera to replace the X-ray film that has many well-know shortenings. Thanks to the axisymmetric microscope and the electronic readout we obtained an immediate viewing of laser driven plasma images.

It is the a powerful tool for experimenters who can rapidly acquire the data necessary to the control of the following laser shots.

References

- /1/ H. WOLTER, Annalen der Physik, Dtsch., 1952, 10, p. 94-114.
- /2/ H. WOLTER, Annalen der Physik, Dtsch., 1952, 10, p. 286-295.
- /3/ R.C. CHASE, J.K. SILK, Applied Optics, 14(9), sept. 1975, p. 2096-2098.
- /4/ M.J. BOYLE, H.G. AHLSTROM, Rev. Sci. Inst., 49(6), jun. 1978, p. 746-750.
- /5/ C. CAVAILLER et al, X-ray CCD imaging device coupled to a pinhole camera, 16th International Congress on High Speed Photography and Photonics, STRASBOURG, FRANCE, august 27-31 1984 (to be published).
- /6/ C. CAVAILLER et al, Electronic readout devices for picosecond streak cameras, same congress.

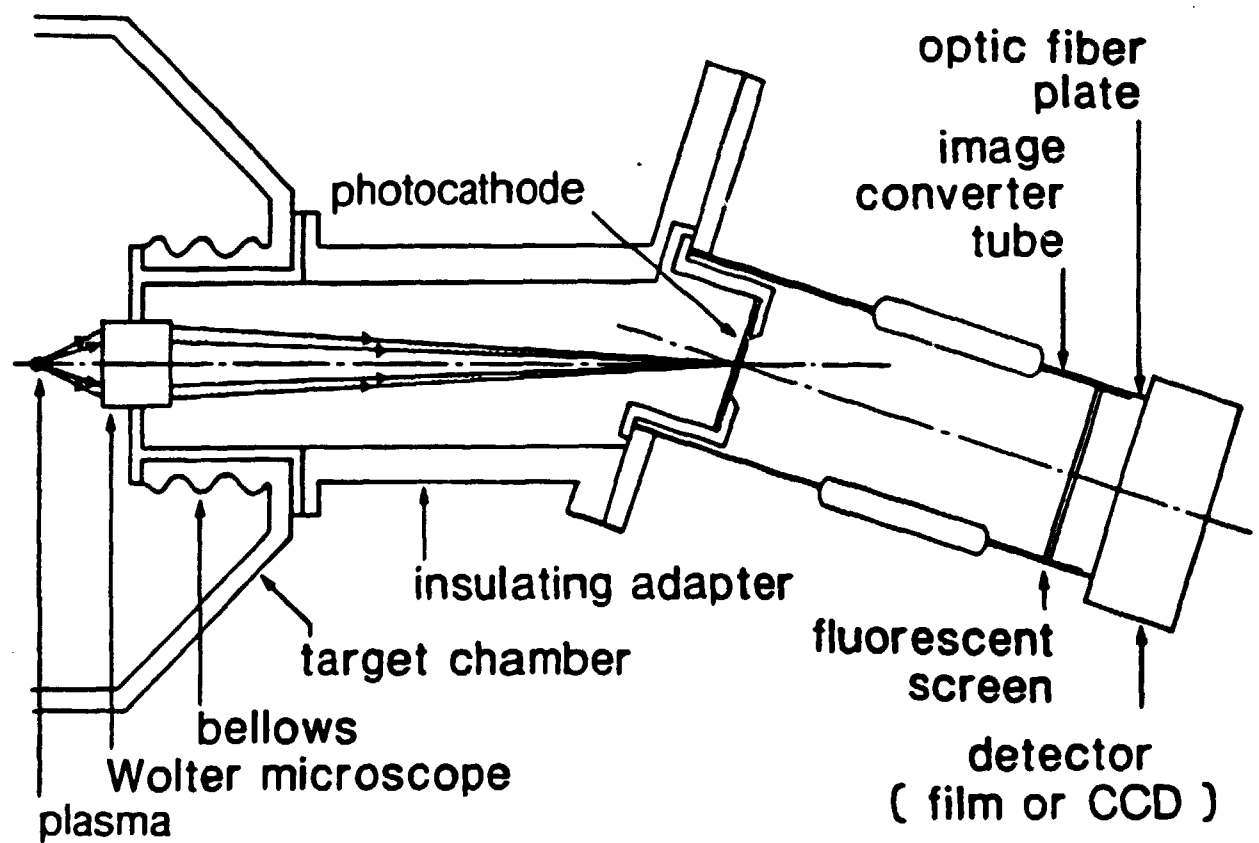


Figure 1 - Schematic representation of an apparatus using an axisymmetric microscope and an electronic image readout

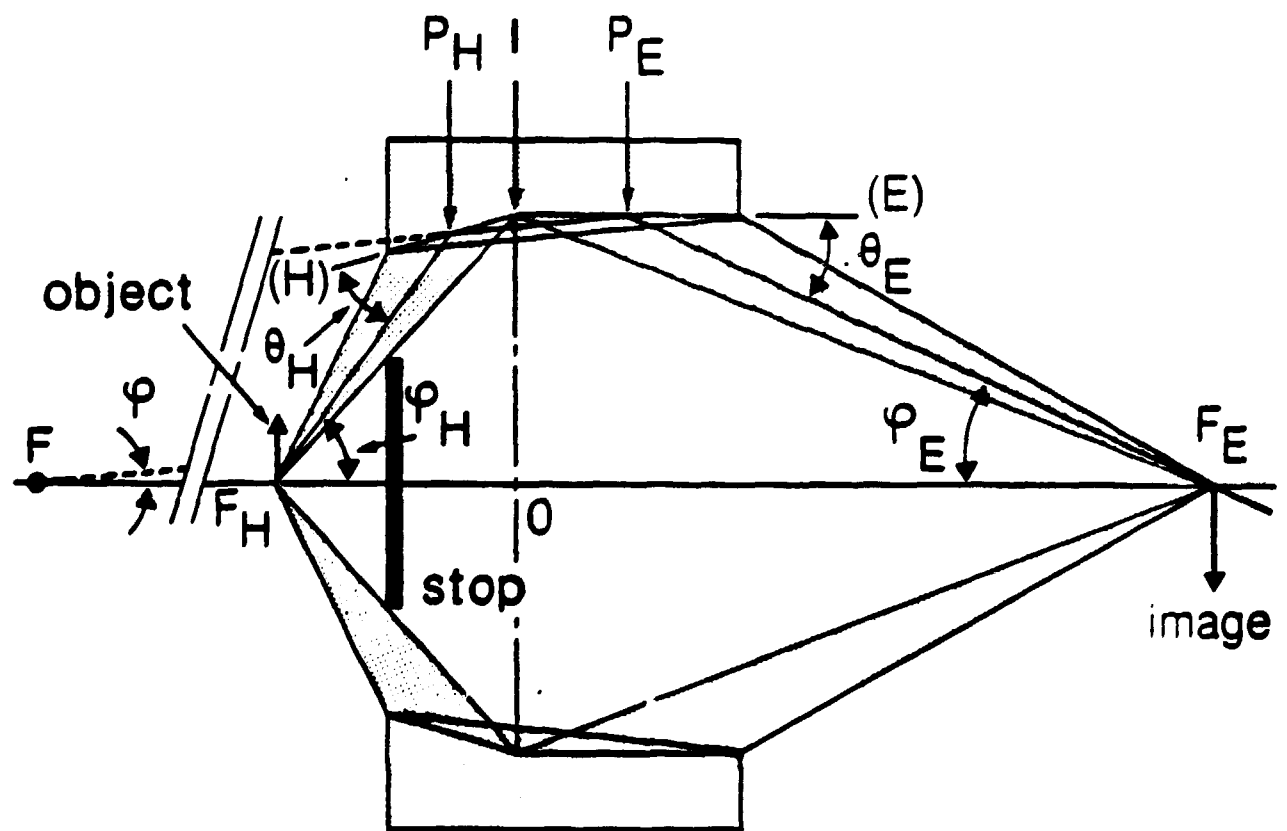


Figure 2 - Principle of an X-ray axisymmetric microscope

Grid periodicity

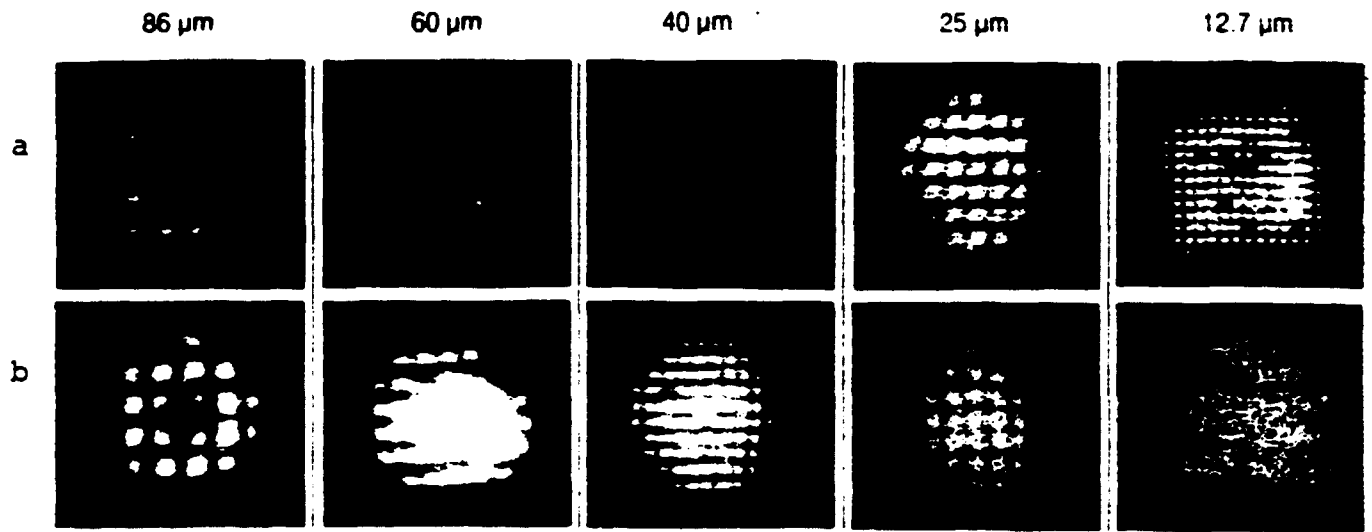


Figure 3 - Resolution tests of the axisymmetric microscope
 a) with visible light
 b) with X-rays

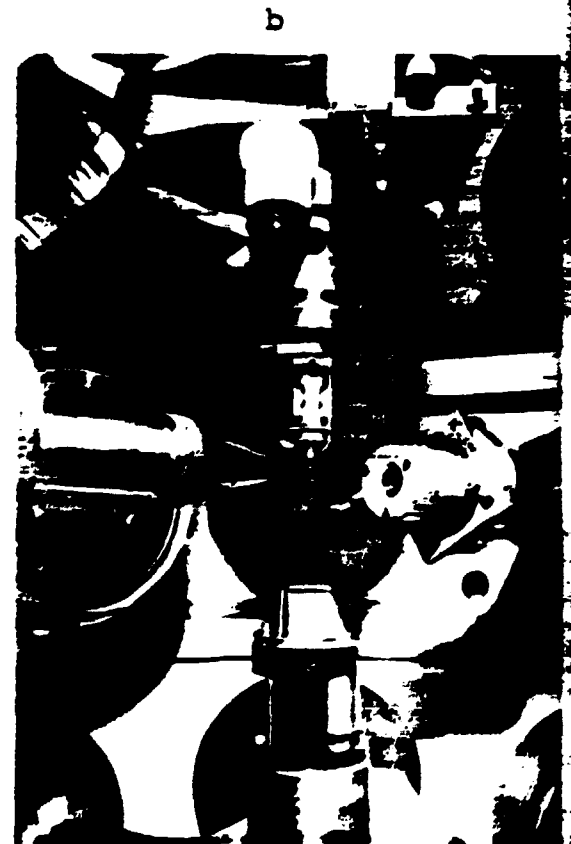
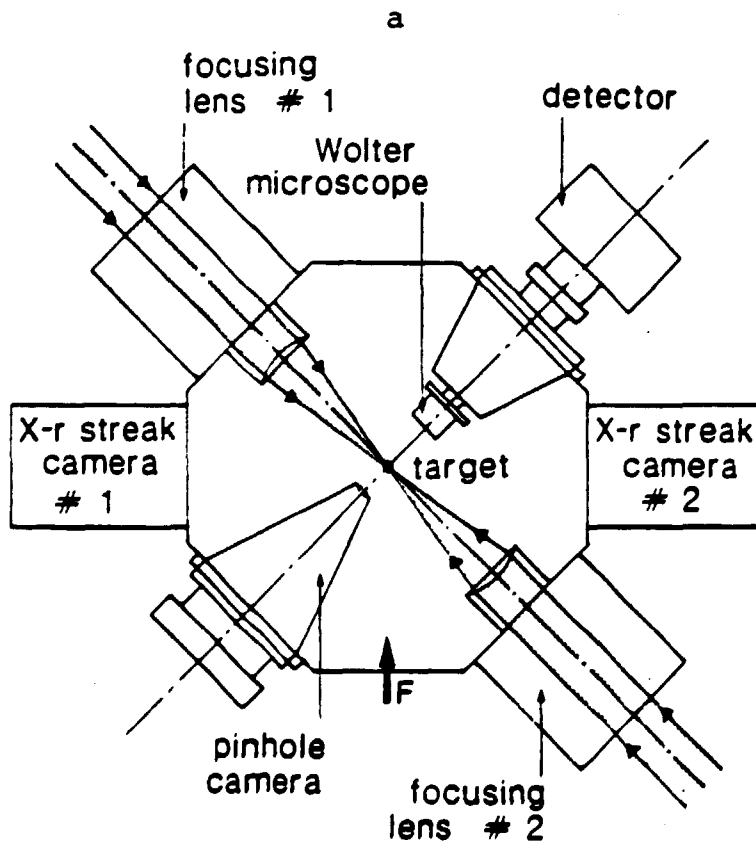


Figure 4 - Experimental set-up for testing the microscope on the pulsed X-ray source
 a) Principle
 b) View according to F direction

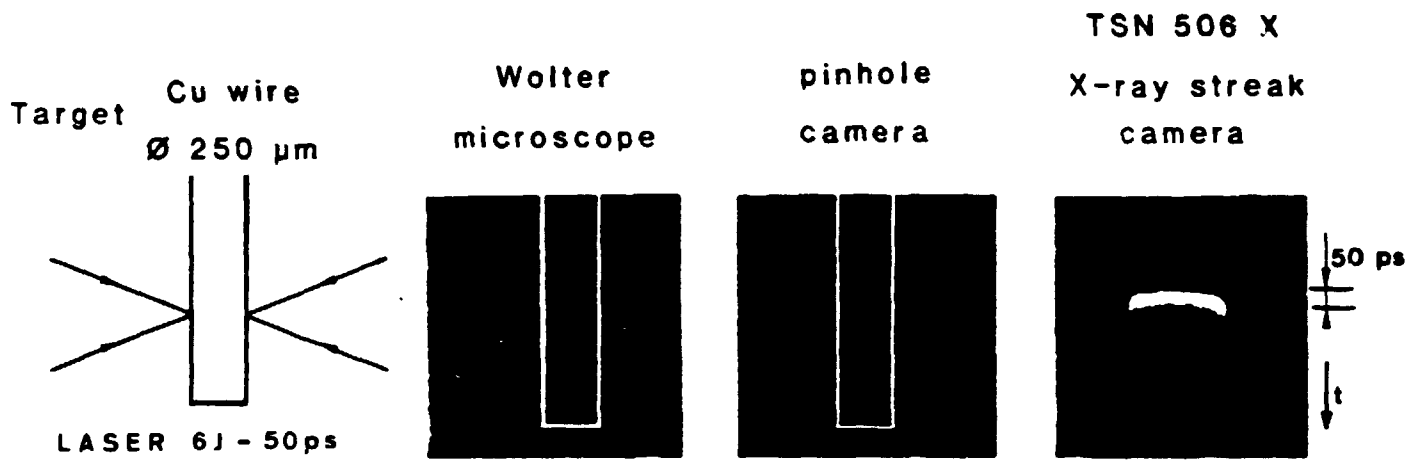


Figure 5 - Double plasma images recorded on X-ray film

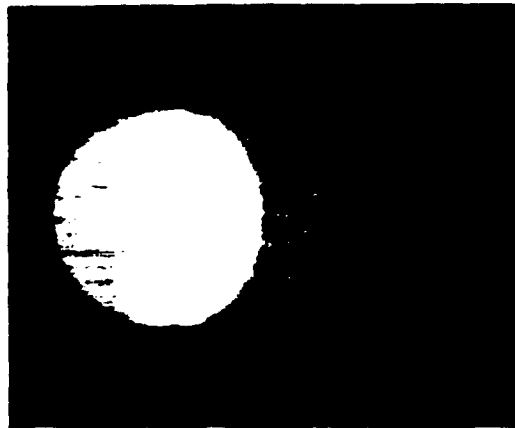


Figure 6 - Spatial resolution test of the ICT (grid period $75 \text{ } \mu\text{m}$)



Figure 7 - Double plasma image given by the microscope and the ICT and recorded on Polaroid 55 PN



Figure 8 - Photograph of the whole apparatus mounted on the interaction chamber

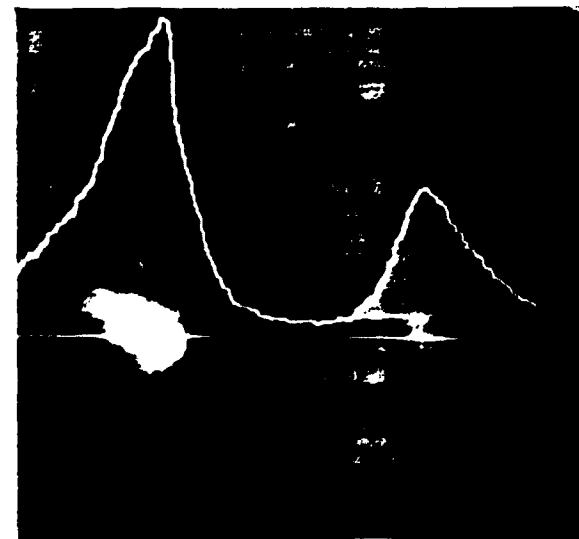


Figure 9 - Image of the X-ray source given by the microscope and recorded by the automatic readout.